From Simple Liquid to Polymer Melt. Glassy and Polymer Dynamics Studied by Fast Field Cycling NMR Relaxometry: Rouse Regime

S. Kariyo,[†] A. Brodin,[§] C. Gainaru,[§] A. Herrmann,[§] J. Hintermeyer,[§] H. Schick,[§] V. N. Novikov,[‡] and E. A. Rössler*,[§]

Faculty of Science and Technology, Yala Islamic University, 135/8 M.3, T. Khaotoom A.Yarang, Pattani 94160, Thailand; IA&E, Russian Academy of Sciences, Novosibirsk 630090, Russia; and Experimentalphysik II, Universität Bayreuth, 95440 Bayreuth, Germany

Received December 11, 2007; Revised Manuscript Received April 23, 2008

ABSTRACT: We apply fast field cycling NMR to study the dispersion of the ^{1}H spin−lattice relaxation time $T_1(\omega)$ of linear 1,4-polybutadienes with molecular weight M (g/mol) ranging from $M = 355$ to 817 000. By this, the crossover from glassy dynamics through Rouse to reptation becomes accessible. Analyzing the data in the susceptibility form $\omega/T_1(\omega)$ and applying frequency−temperature superposition, spectra extending over up to 8 decades in ω are obtained. Characteristic polymer spectra are revealed when the underlying glassy dynamics are accounted for. Instead of describing the unentangled melt by the full Rouse mode spectrum, the emergence of a limited number of modes is identified which saturates when entanglement sets in. A quantitative analysis yields the molecular weight of a Rouse unit $M_R \cong 500$, and the entanglement weight $M_e \cong 2000$, at which first entanglement effects are observed. Moreover, the dynamic order parameter $S(M)$ and the behavior of the terminal time $\tau_{max}(M)$ are obtained. Both quantities allow to identify three dynamic regimes, namely simple liquid, Rouse, and reptation dynamics. The temperature dependence of the segmental relaxation time $\tau_s(T)$ coincides with the corresponding dielectric relaxation times which were measured additionally, and the M dependence of the glass transition temperature T_g shows distinctive kinks at M_R and M_e, indicating that glassy dynamics are modified by polymer dynamics.

I. Introduction

In the preceding contribution,[1] hereafter called paper I, and in a preliminary study,[2] we investigated the frequency dispersion of the ^{1}H spin−lattice relaxation time $T_1(\omega)$ of different 1,4-polybutadienes (PB) over a large temperature range in the limits of high ($M = 56\,500-817\,000$ g/mol) as well as low molecular weight ($M = 355$ and 466 g/mol). The dispersion of T_1 was determined from fast field cycling (FFC) NMR experiments, performed with a spectrometer STELAR FFC 2000.[3,4] Such spectrometers became only recently available and allow to access in particular slow modes in soft matter which otherwise may be difficult to probe.

To a fair approximation, dispersion of the ^{1}H spin−lattice relaxation time reflects the spectrum of orientational dynamics of a polymer segment. In addition to local segmental dynamics with time constant τ_s that corresponds to the structural α relaxation ($\tau_s = \tau_\alpha$), polymer segmental motion also reflects much slower collective chain dynamics.[3,4] Assuming frequency−temperature superposition (FTS), we combined the spectra of different temperatures so as to effectively cover about 6 orders at $\omega\tau_s < 1$, where Rouse and entanglement effects[5,6] are expected. As shown in paper I, PB oligomers with $M \leq 500$, i.e., with only a few repeat units, behave similarly to simple liquids such as *o*-terphenyl in that they only exhibit α-relaxation, characteristic of the glass transition,[7−9] but no polymer effects. In contrast, high-M PB samples show additional, polymer-specific relaxation related to Rouse and reptation dynamics. We further argued that, in order to properly access quantitative aspects of the spectral contributions due to polymer-specific dynamics (denoted "polymer spectra" in the following), the generally stronger contribution of local, segmental motions ("glassy dynamics") has to be accounted for.

To facilitate analyses and comparisons with other techniques, it is convenient to rewrite the Bloembergen, Purcell, Pound (BPP)[10,11] expression for the relaxation rate $1/T_1$ in the susceptibility form[2]

$$\omega/T_1 = C[\chi''(\omega) + 2\chi''(2\omega)] \equiv 3C\bar{\chi}''(\omega) \quad (1)$$

where C is the NMR coupling constant and $\chi''(\omega) = \omega J(\omega)$ the susceptibility, with the spectral density $J(\omega)$ that is approximately given by the Fourier transform of the second rank orientational correlation function $F_2(t)$ of a polymer segment (see paper I). Assuming statistical independence and additivity of the contribution by glassy and polymer dynamics, we write

$$\bar{\chi}''(\omega) = (1 - S^2)\bar{\chi}''_{glass}(\omega) + S^2\bar{\chi}''_{polymer}(\omega) \quad (2)$$

where S is the "dynamic order parameter"[12−15] (see paper I for a discussion of S), so that the relaxation strength $f = S^2$ is the amount of orientational correlation relaxed via polymer dynamics alone. In the case of simple liquids, polymer dynamics is absent, i.e., $S \equiv 0$. In most polymers, the slow reptation dynamics occur at such low frequencies where $\tilde{\chi}''_{glass}(\omega)$ may be ignored, so that $\tilde{\chi}''_{polymer}(\omega)$ dominates the spectrum. The intermediate Rouse dynamics, however, partly overlap with $\tilde{\chi}''_{glass}(\omega)$, so that close to the α-relaxation peak the total spectrum cannot be assumed to reflect polymer dynamics alone. This is especially true, since the contribution of polymer dynamics is relatively weak, $S^2 \ll 1$. Thus, interpreting FFC NMR relaxation data of polymers without accounting for the underlying glass spectrum may be misleading.

In paper I, we determined the limiting behavior of PB in the cases of low and high molecular weight. In the current contribution, we study the crossover between these limits, investigating a range of molecular weights $355 \leq M_w \equiv M \leq 817\,000$ (see Table 1). The analysis proceeds along the lines of part I, whereby polymer contributions are extracted from the total spectrum by subtracting the glassy part (see eq 2). Recalling that low-M PB oligomers are akin to simple molecular liquids,

* Corresponding author.
[†] Yala Islamic University.
[‡] Russian Academy of Sciences.
[§] Universität Bayreuth.

10.1021/ma702758j CCC: $40.75
Published on Web 06/26/2008

Table 1. Details of the Measured Polybutadiene (PB) Samples[a]

sample name	M_w [g/mol]	M_n [g/mol]	polydispersity M_w/M_n	T_g [K]
PB355	355	335	1.06	140.9
PB466	466	437	1.06	161.2
PB575[b]	575	543	1.06	162.1
PB777	777	732	1.06	165.3
PB1450	1450	1350	1.08	170.7
PB2020	2020	1890	1.07	173.6
PB2760	2760	2640	1.05	174.4
PB4600	4600	4470	1.03	174.0
PB11400	11400	11100	1.03	
PB19900[b]	19900	19300	1.03	175.3
PB35300[b]	35300	34700	1.02	174.5
PB56500	56500	55500	1.02	
PB87000	87000	86000	1.01	174.4
PB314000	314000	308000	1.02	
PB817000	817000	774000	1.05	

[a] Note that the name of the PB samples reflects its molecular weight M_W. Systems for which T_g is listed were measured by dielectric spectroscopy. [b] Measured only by dielectric spectroscopy.

whereas high-M polymers additionally exhibit Rouse and reptation effects, we expect that Rouse dynamics starts to emerge, when the chain length exceeds the Rouse unit size M_R, whereas the development of Rouse dynamics is eventually modified, or effectively truncated, by entanglement effects above the entanglement weight $M > M_e$. We will indeed demonstrate these crossovers in the polymer spectra. We also estimate the molecular weight dependence of the order parameter $S(M)$.

We use in addition dielectric spectroscopy to determine the segmental time constant $\tau_s(T)$, which we compare with the corresponding results of FFC NMR and which allows to determine the glass transition temperature T_g. Examining the molecular weight dependence of T_g, we found in our preliminary study[2] distinct kinks at M_R and M_e in the $T_g(M)$ dependence, which appears to challenge the results of many studies that report a continuous change of $T_g(M)$ described by free volume theory.[16,17] We note, however, that an early work of Cowie[18] already reported pronounced kinks in $T_g(M)$. The literature results are thus contradictory. We shall however show, based on our results of PB, that the glass transition in a polymer is related to the characteristic polymer dynamics, whose distinctive molecular weight dependence is reflected also in the corresponding dependence of $T_g(M)$.

The paper is organized as follows. In section II, we summarize the results of the Rouse theory in relation to the second-rank segmental orientational correlation function $F_2(t)$, whose Fourier transform is determined in FFC NMR experiments. In particular, we discuss the short-chain limit, where only a few Rouse modes exist. Section III briefly repeats some of the experimental details discussed in paper I. Experimental results are presented in section IV and discussed in section V.

II. Theoretical Background: Spin−Lattice Relaxation Analyzed in the Frame of the Rouse Theory

Dynamics of relatively short, nonentangled polymer chains in a melt may be described by the Rouse model.[19] It is assumed that the chains are Gaussian and sufficiently long, so that they can be further subdivided into Gaussian segments. The chain is then represented by N "beads" of mass M_R, immersed in an effective viscous medium and connected by $N - 1$ mass less entropic springs. It is further assumed that viscous damping is sufficiently large, so that inertial effects are unimportant. Solving the corresponding eigenvalue problem then yields N orthogonal relaxation modes $p = 0, 1,..., N - 1$ ($p = 0$ corresponds to uniform translation not considered here) with relaxation times (eigenvalues) τ_p and normal coordinates (eigenvectors) $\mathbf{X}_p(t)$, the so-called Rouse modes

$$\mathbf{X}_p(t) = \frac{1}{N}\sum_{n=1}^{N} \mathbf{R}_n(t) \cos\left(\frac{p\pi(n-1/2)}{N}\right) \tag{3}$$

where $\mathbf{R}_n(t)$ is the position vector of nth bead. The correlation functions of Rouse normal modes $\mathbf{X}_p(t)$ are then[19−21]

$$C_p(t) = \langle \mathbf{X}_p(t)\, \mathbf{X}_p(0)\rangle = \frac{b^2}{8N \sin^2(p\pi/2N)} \exp(-t/\tau_p) \qquad p = 1, \ldots, N-1 \tag{4}$$

and b the effective Rouse segment length. The relaxation time τ_p of the pth mode is

$$\tau_p = \frac{\tau_0 \pi^2}{4 \sin^2(p\pi/2N)} \tag{5}$$

with $\tau_0 = b^2\zeta/(3\pi^2 kT)$, where ζ is the friction coefficient of a bead. The longest relaxation time τ_R (the Rouse time), corresponding to $p = 1$, is then given by

$$\tau_R = \frac{\tau_0 \pi^2}{4 \sin^2(\pi/2N)} \tag{6}$$

For long chains with $N \gg 1$, the essential part of the polymer dynamics comes from the modes with $p/N \ll 1$. In this case, the sine in eqs 4–6 can be substituted by its argument, and then, the parameters of the Rouse dynamics assume the form most often found in the literature[5,22]

$$C_p(t) \approx \frac{Nb^2}{2\pi^2 p^2} \exp(-t/\tau_p), \qquad \tau_p \cong \tau_0 N^2/p^2 \text{ and } \tau_R \cong \tau_0 N^2 \quad (0 < p \ll N) \tag{7}$$

This approximation was used, in particular, in our preliminary work.[2] It is, however, a poor approximation for relatively short chains with only a few Rouse modes. We therefore use the exact eqs 4–6 in the following.

According to Bloembergen, Purcell, and Pound,[3,4,10,11] the NMR spin−lattice relaxation time T_1 of macroscopically isotropic samples is expressed in terms of the spectral density $J(\omega)$, related to the second rank orientational correlation function, as (cf. also eq 1)

$$\frac{1}{T_1} = C[J(\omega) + 4J(2\omega)] \tag{8}$$

For a Rouse chain, the relevant correlation function is the one of the polymer segments, so that the spectral density can be approximated by[3,23−26]

$$J(\omega) \propto \int_{-\infty}^{\infty} \mathrm{d}t\, \mathrm{e}^{i\omega t} \langle \mathbf{b}(t)\, \mathbf{b}(0)\rangle^2 / b^4 \tag{9}$$

where

$$\langle \mathbf{b}(t)\, \mathbf{b}(0)\rangle = \frac{1}{N-1}\sum_{n=1}^{N-1} \langle \mathbf{b}_n(t)\, \mathbf{b}_n(0)\rangle \tag{10}$$

In eqs 9 and 10, $\langle \mathbf{b}(t)\, \mathbf{b}(0)\rangle$ is the correlation function of the chain tangent vector averaged over the chain and $\mathbf{b}_n(t)$ is the Rouse segment vector of the nth segment of the chain, $\mathbf{b}_n(t) = \mathbf{R}_{n+1}(t) - \mathbf{R}_n(t)$. Expressing $\mathbf{R}_n(t)$ via the normal modes $\boldsymbol{X}_p(t)$

$$\mathbf{R}_n(t) = \mathbf{X}_0(t) + 2\sum_{p=1}^{N-1} \mathbf{X}_p(t) \cos\left(\frac{p\pi(n-1/2)}{N}\right) \tag{11}$$

one obtains

$$\langle \mathbf{b}(t)\,\mathbf{b}(0)\rangle = \frac{4}{N-1}\sum_{n,p=1}^{N-1}\langle \mathbf{X}_p(t)\,\mathbf{X}_p(0)\rangle \times \left[\cos\left(\frac{p\pi(n+1/2)}{N}\right)-\cos\left(\frac{p\pi(n-1/2)}{N}\right)\right]^2 = \frac{16}{(N-1)}\sum_{p=1}^{N-1} C_p(t)\sin^2(p\pi/2N)\sum_{n=1}^{N-1}\sin^2(p\pi n/2N) \quad (12)$$

The last sum over n is equal to $N/2$ and, in fact, does not depend on p. As a result, taking into account expression 4 for $C_p(t)$, one has

$$\langle \mathbf{b}(t)\,\mathbf{b}(0)\rangle = \frac{b^2}{N-1}\sum_{p=1}^{N-1}\exp(-t/\tau_p) \quad (13)$$

Respectively

$$J_{\text{Rouse}}(\omega) = \text{Re}\,\frac{1}{(N-1)^2}\int_{-\infty}^{\infty} \mathrm{d}t\, e^{i\omega t}\sum_{p,q=1}^{N-1}\exp(-|t|/\tau_{pq}) \quad (14)$$

Here

$$\tau_{pq}^{-1} = \tau_p^{-1}+\tau_q^{-1} = \frac{4}{\pi^2\tau_0}\left[\sin^2\left(\frac{p\pi}{2N}\right)+\sin^2\left(\frac{q\pi}{2N}\right)\right] \quad (15)$$

$$= \tau_0^{-1}(p^2+q^2)/N^2 \quad \text{at } p/N, q/N \ll 1 \quad (15a)$$

After integration, eq 14 gives the following expression for $J(\omega)$

$$J_{\text{Rouse}}(\omega) = \frac{1}{(N-1)^2}\sum_{p,q=1}^{N-1}\frac{\tau_{pq}^{-1}}{\tau_{pq}^{-2}+\omega^2} = \frac{4\tau_0}{\pi^2(N-1)^2}\sum_{p,q=1}^{N-1}\frac{\sin^2\left(\frac{p\pi}{2N}\right)+\sin^2\left(\frac{q\pi}{2N}\right)}{\frac{16}{\pi^4}\left[\sin^2\left(\frac{p\pi}{2N}\right)+\sin^2\left(\frac{q\pi}{2N}\right)\right]^2+\omega^2\tau_0^2} \quad (16)$$

$$= \tau_0\sum_{p,q=1}^{N-1}\frac{p^2+q^2}{(p^2+q^2)^2+\omega^2\tau_R^2} \qquad \text{for } N \gg 1 \quad (16a)$$

In eq 16 $J_{\text{Rouse}}(\omega)$ is normalized in such a way that its integral is equal to $\pi/2$:

$$\int_0^{\infty} J_{\text{Rouse}}(\omega)\,\mathrm{d}\omega = \pi/2 \quad (17)$$

We will be interested, in particular, in the magnitude of spectral density at $\omega = 0$. From eq 16 it follows that

$$J_{\text{Rouse}}(0) = \frac{1}{(N-1)^2}\sum_{p,q=1}^{N-1}\tau_{pq} = \frac{1}{(N-1)^2}\sum_{p,q=1}^{N-1}\frac{\tau_p\tau_q}{\tau_p+\tau_q} = \langle\tau\rangle \quad (18)$$

At $N \gg 1$, the sum in eq 16 can be represented as an integral. Introducing new variables $p = r\cos\varphi$ and $q = r\sin\varphi$, so that $p^2 + q^2 = r^2$, one obtains

$$J_{\text{Rouse}}(\omega) \cong (\tau_0/2)\int_0^{\pi/4}\mathrm{d}\varphi\,\ln\left(\frac{1+\omega^2\tau_0^2\cos^4\varphi}{1+\omega^2\tau_R^2\cos^4\varphi}N^4\right), \quad N \gg 1 \quad (19)$$

This spectral density has two characteristic frequency regimes. At small frequencies, less than the inverse Rouse time $\omega \ll \tau_R^{-1}$, since $\omega\tau_0$, $\omega\tau_R \ll 1$, one can neglect the frequency-dependent terms under the integral eq 19. As a result, at small frequencies $J_{\text{Rouse}}(\omega)$ is a constant, as in the Debye case,[24] its numerical value depending on ln N:[3]

$$J_{\text{Rouse}}(\omega) = J_{\text{Rouse}}(0) = (\pi\tau_0/2)\ln N \qquad \omega\tau_0, \omega\tau_R \ll 1 \quad (20)$$

At intermediate frequencies $\tau_R^{-1} \ll \omega \ll \tau_0^{-1}$, i.e., in the Rouse regime, one can neglect $\omega^2\tau_0^2\cos\varphi$ in the numerator and unity in the denominator of the integral eq 19. As a result, $J_{\text{Rouse}}(\omega)$ is a logarithmic function of frequency

$$J_{\text{Rouse}}(\omega) \cong \tau_0\int_0^{\pi/4}\mathrm{d}\varphi\,\ln\left(\frac{1}{\omega\tau_0\cos^2\varphi}\right) \quad (21)$$

$$= (\pi/4)\tau_0\ln(a/\omega\tau_0), \quad \omega\tau_0 \ll 1 \ll \omega\tau_R \quad (22)$$

Here, the constant a is defined by the expression

$$\ln a = -\frac{8}{\pi}\int_0^{\pi/4}\mathrm{d}\varphi\,\ln\cos\varphi \cong 0.220 \quad (23)$$

so that $a \cong 1.246$. The expression eq 22 was first derived in ref 23 (cf. also refs 24 and 25).

In Figure 1a we show the spectral density $\tilde{J}_{\text{Rouse}}(\omega) = [J_{\text{Rouse}}(\omega) + 4J_{\text{Rouse}}(2\omega)]/3$ for several values of N. As one can see, the plateau value at the lowest frequencies increases with the chain length N. In addition, we show in Figure 1b the calculated Rouse spectra in the susceptibility representation $\tilde{\chi}''_{\text{Rouse}}(\omega) = \chi''(\omega) + 2\chi''(2\omega)]/3 = \omega\tilde{J}_{\text{Rouse}}(\omega)$. Here, one recognizes an increasing magnitude with the chain length N of the spectra at the lowest frequencies reflecting the redistribution of spectral intensity to lower frequencies. Finally, Figure 1c presents the susceptibility spectra of Figure 1b shifted along the frequency axis such that the spectra agree at lowest frequencies; i.e., the susceptibility is plotted as a function of $\omega\langle\tau\rangle$ (cf. eq 18). This representation shows again the increasing spread of the distribution of correlation times involved in the Rouse spectrum. Equation 20 provides an expression for the Rouse spectrum in the limit of high N. The corresponding curve is included in Figure 1b. This limiting expression reproduces the actual Rouse spectrum only for N, say, larger than 100 that, as will be shown below, cannot be achieved experimentally as entanglement sets in at much lower N. In Figure 2, the dependence of $J_{\text{Rouse}}(0)$ on N (eq 18) is shown as a function of N. At large N, a linear behavior is observed. At small N, deviations from the asymptotic linear behavior are recognized.

Later, we will compare the results of eq 16 and 18 to the experimental FFC NMR relaxation data. A quantitative comparison, however, is only possible when the spectrum of the polymer dynamics is extracted from the overall relaxation spectrum; here eq 2 will be applied. In order to map the results from the Rouse theory given as a function of the chain length $N = M/M_R$, the Rouse unit molecular mass M_R appears as a fitting parameter. Moreover, in accordance with refs 3 and 4, we identify the time τ_0 fixed by the local friction coefficient with the segmental relaxation time τ_s which is provided by shifting the susceptibility data along the frequency axis to obtain a master curve.

III. Experimental Section

Details of FFC NMR experiments have been already presented in paper I. Table 1 lists the 1,4-polybutadiene (PB) samples, characterized in the present work, and their properties. All the samples were purchased from Polymer Standards Service, Mainz, Germany. Throughout the paper, M refers to the weight-average M_w, expressed in g mol^{-1}. The glass transition temperature T_g is defined as the temperature, at which dielectric relaxation time equals 100 s. For details of the dielectric results and their analyses, see paper I.

IV. Results

A. Overall Dispersion Spectra. In Figure 3a, we show frequency-dependent NMR relaxation time data of a PB sample with $M = 4600$. We expect that this relatively short polymer is

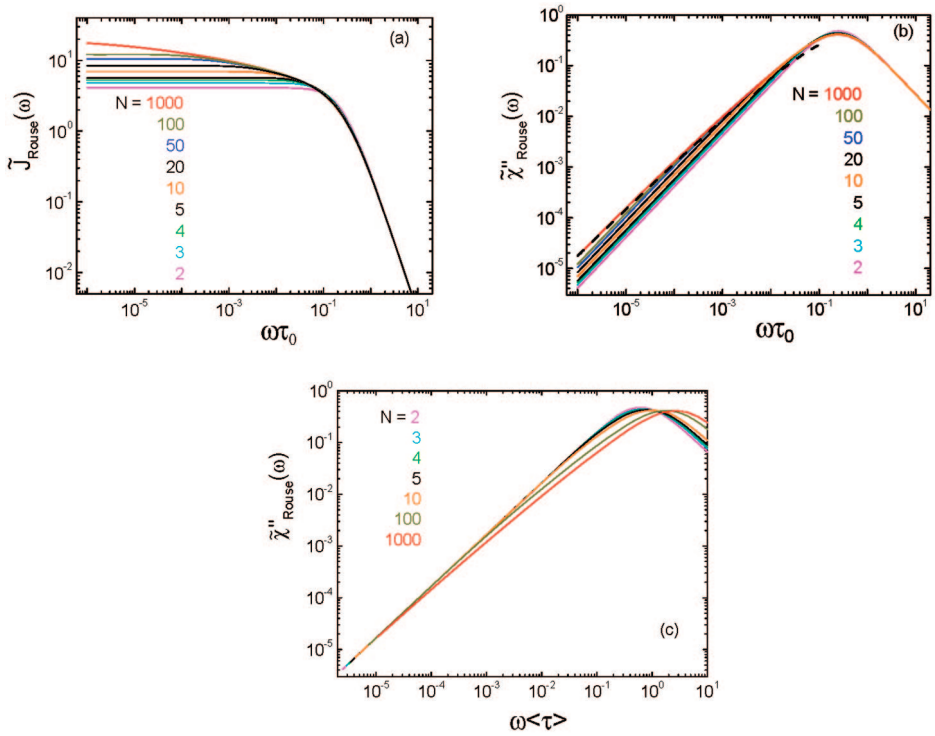

Figure 1. (a) Normalized NMR spectral density $\tilde{J}_{Rouse}(\omega)$ (cf. eq 1) calculated within Rouse theory for several chain lengths N as indicated; τ_0 denotes the shortest Rouse time (cf. eq 5). (b) The corresponding NMR susceptibility $\tilde{\chi}''_{Rouse}(\omega)$ (cf. eq 1); included is the high N limit of the Rouse spectrum (dashed line), cf. eq 22. (c) Rouse susceptibility spectra scaled to agree at lowest frequencies.

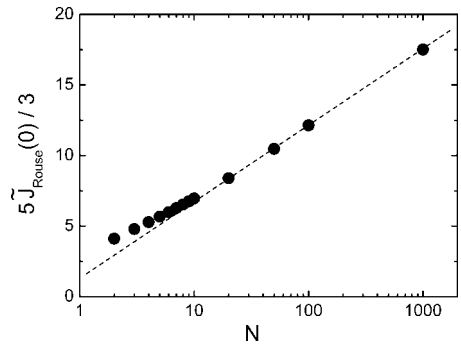

Figure 2. NMR spectral density in the low-frequency limit, $\omega\tau_R \ll 1$, as a function of N; dashed line represents extrapolation of the high N limit, according to eq 20.

still long enough for Rouse dynamics to develop. Indeed, the spectra in the susceptibility representation of Figure 3b deviate from the simple liquid limit $\tilde{\chi}''(\omega) \propto \omega$ at $\omega\tau_s \ll 1$(dashed line) and thus reveal the polymer effect. Note that at certain temperatures the spectra of Figure 3b exhibit a maximum, which is identified with the α-relaxation peak; i.e., at the maximum the condition $\omega\tau_s \cong 1$ holds. As discussed in paper I, a master curve can be constructed by shifting all the dispersion spectra for the different temperatures along the frequency axis to collapse on a single curve $\tilde{\chi}''(\omega\tau_s)$. In order to provide not only shift factors but absolute correlation times τ_s, the master curve, e.g., for PB4600, is shifted such as to agree on the high-frequency side ($\omega\tau_s \geq 1$) with the corresponding master curve of the low-M systems PB466 or PB355. The latter systems do not show any signs of polymer dynamics, so that their susceptibility curves fully coincide at $\omega\tau_s < 1$ with that of the glass-former *o*-terphenyl, and the susceptibility can be fitted with an appropriate spectral function to yield the time constant τ_s (cf. paper I). This procedure involves the validity of frequency−temperature superposition (FTS). In particular, in the case of polymers this assumes that glassy and polymer dynamics show the same temperature dependence. Though often applied in polymer physics, this may fail close to T_g,[27,28] but FFC NMR probes the dynamics well above T_g.

The result of this procedure is shown in Figure 4 together with the data of low-M PB355 and PB466 from paper I, and the difference is attributed to the spectral contribution of polymer dynamics of PB4600. Note that at lowest frequencies the susceptibility of PB4600 is linear in frequency (dashed line), as in the low-M liquids. This indicates that the Rouse or terminal time is reached, so that the full range of polymer (Rouse) spectrum is covered. The procedure of obtaining master curves was then repeated for the other PB samples. Figure 5 displays their relaxation times, obtained during construction of the master curves, together with the corresponding dielectric relaxation times. As in the cases already discussed in paper I, the dielectric and NMR relaxation times agreeably match, which is a justification of FTS. Thus, in what follows, the master curves, significantly extending the accessible frequency range, are taken to identify the spectral contributions from glassy as well as polymer dynamics. In paper I we also showed that $\tau_s(T)$ are the same for the high-M samples PB56500, PB87000, PB314000, and PB817000.

Figure 6a presents the master curves $\tilde{\chi}''(\omega\tau_s)$ of all PB samples, from $M = 355$ up to 817 000. Increasing molecular weight beyond $M = 466$ brings about excess intensity at $\omega\tau_s < 1$ with respect to $\tilde{\chi}''(\omega\tau_s) \propto \omega^1$ (simple liquid limit, cf Paper I), which progressively grows until at $M \geq 56\,500$ the spectra become independent of M, indicating that the entanglement in the polymer melt is fully developed, as far as the Rouse spectrum that we observe is concerned. We note that the related reptation dynamics that emerge in the entangled polymer melt are of course M-dependent but too slow to be fully detected in the accessible frequency window. Yet, the upturn of the upper ($M > 11\,400$) traces in Figure 6a at the lowest frequencies is not compatible with the expected Rouse behavior, so that it must be related to reptation dynamics (cf. subsection B). Still, for $M \leq 11\,400$ we observe the limiting behavior $\tilde{\chi}''(\omega\tau_s) \propto \omega^1$at the

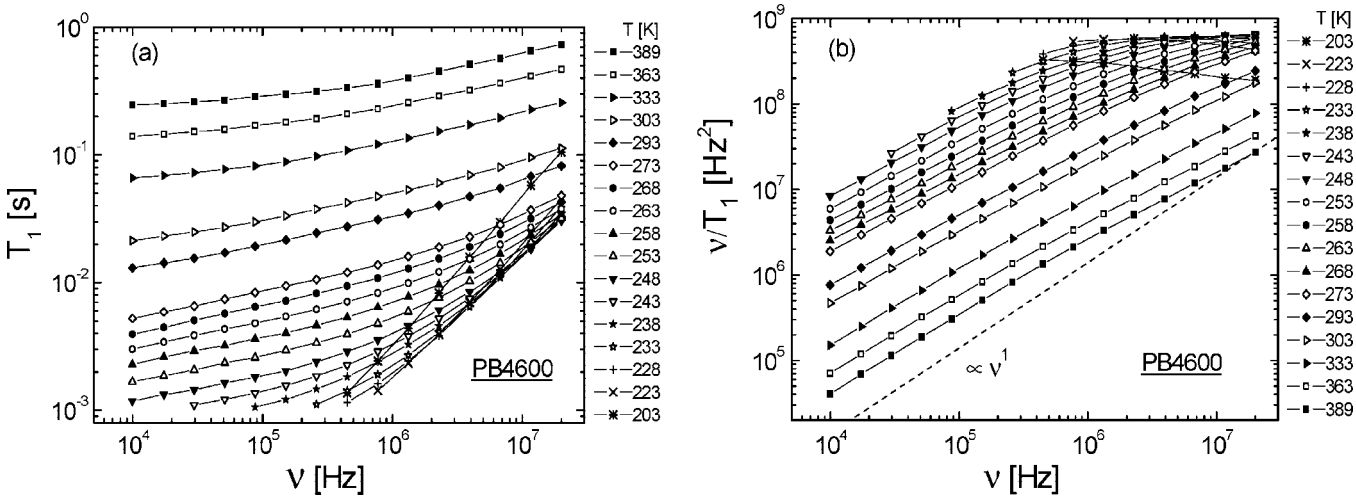

Figure 3. (a) Spin−lattice relaxation time T_1 as a function of frequency ν for 1,4-polybudadiene with molecular weight $M = 4600$ (PB4600) at different temperatures as indicated; lines: guide for the eye. (b) Susceptibility representation of the dispersion data in (a); dashed straight line: power law behavior as expected for simple liquids at $\omega\tau_s < 1$.

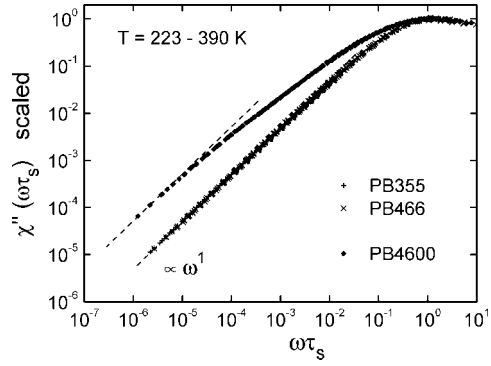

Figure 4. Master curves for the NMR susceptibility obtained for three 1,4-polybutadiene samples with molecular weight as indicated (numbers); experimental spectra in the temperature range indicated are used; dashed lines show Debye behavior at low frequencies.

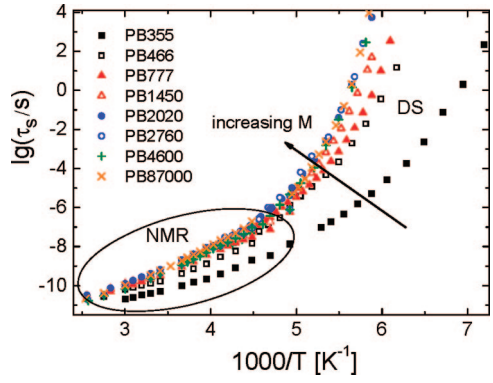

Figure 5. Comparison of segmental time constant τ_s as obtained by FFC NMMR and dielectric spectroscopy (DS). Time constant as a function of reciprocal temperature for the polybutadiene samples with different molecular weight M (as indicated); circle indicates range for which FFC NMR provides information, and beyond the circle the data are taken from the DS spectra.

lowest frequencies of Figure 6a, which means that even for this relatively high-M sample the slowest relaxation with $\tau = \tau_{max}$ is fully detected.

The existence of a limiting $\tilde{\chi}''(\omega\tau_s) \propto \omega^1$ behavior implies that the spectra at higher M may be rescaled, so that they overlap with the lower M spectra at low frequencies. Such rescaled spectra are plotted in Figure 6b. Two features are recognized in this representation of the data. First, the crossover to a linear $\tilde{\chi}''(\omega\tau_s) \propto \omega^1$ behavior, characterizing the "end" of the polymer dynamics at low frequencies, shifts left (becomes slower) with increasing M (crossover points are marked with arrows in Figure 6b). Next, whereas for $M \leq 2760$ the spectra are only broadened at the low-frequency side at $\omega\tau_s < 1$, the spectrum for $M = 11\,400$ (and marginally at $M = 4600$) exhibits a bimodal structure which can already be anticipated in Figure 4. We interpret it as an indication of entanglement effects that are first discernible at $M = 4600$. The ratio τ_{max}/τ_s may be estimated from Figure 6a,b. In Figure 7 its M dependence is presented. Whereas for $M \leq 466$ no dependence on M is recognized within the accuracy of the FFC experiments, at $777 \leq M \leq 2000$, the dependence resembles $\tau_R \propto M^2$ of the Rouse relaxation time (see eq 7). At still higher M, the $\tau_{max}(M)$ dependence appears closer to $\propto M^3$, as expected in the entanglement regime.[5,6] The crossover between the two regimes occurs indeed at a characteristic molecular weight of $M_e \cong 2000$.

As an alternative way to present the data in the susceptibility representation $\tilde{\chi}''(\omega\tau_s)$, we transform them into the corresponding segmental orientational correlation functions $\tilde{F}_2(t)$ (neglecting again the difference of $J(\omega)$ and $J(2\omega)$ (see Figure 8). A meaningful transformation that is relatively free from low-frequency truncation errors is only possible for the spectral data that show the limiting $\propto \omega^1$ behavior at low frequencies, i.e., for $M \leq 11\,400$. The reorientational correlation function is monitored over 6 decades in amplitude. In going from low $M = 355$ to high $M = 11\,400$, the correlation function becomes increasingly stretched. At $M = 11\,400$, the correlation function appears even bimodal, with a well-defined second "step" at long times. Clearly, polymer effects lead to a retardation of the final relaxation, as full orientational relaxation of a segment is only possible in the course of the slow chain dynamics, viz. Rouse modes and reptation. Even though the $M = 11\,400$ correlation function is two-step, its second part is not slow enough to be clearly separated from the first step by a plateau. At larger M the plateau would eventually appear, the associated entanglement effects being however too slow for our experimental method. The plateau value would directly reflect the dynamic order parameter $f_e = S_e^2$ caused solely by entanglement effects (see eq 2). As will be discussed below, such a plateau is actually not expected when only Rouse dynamics are present. Trying to estimate the order of magnitude of the plateau by fitting the long time decay to a stretched exponential with stretching parameter $\beta = 0.5$, we find a quite low value $f_e = 0.0006$

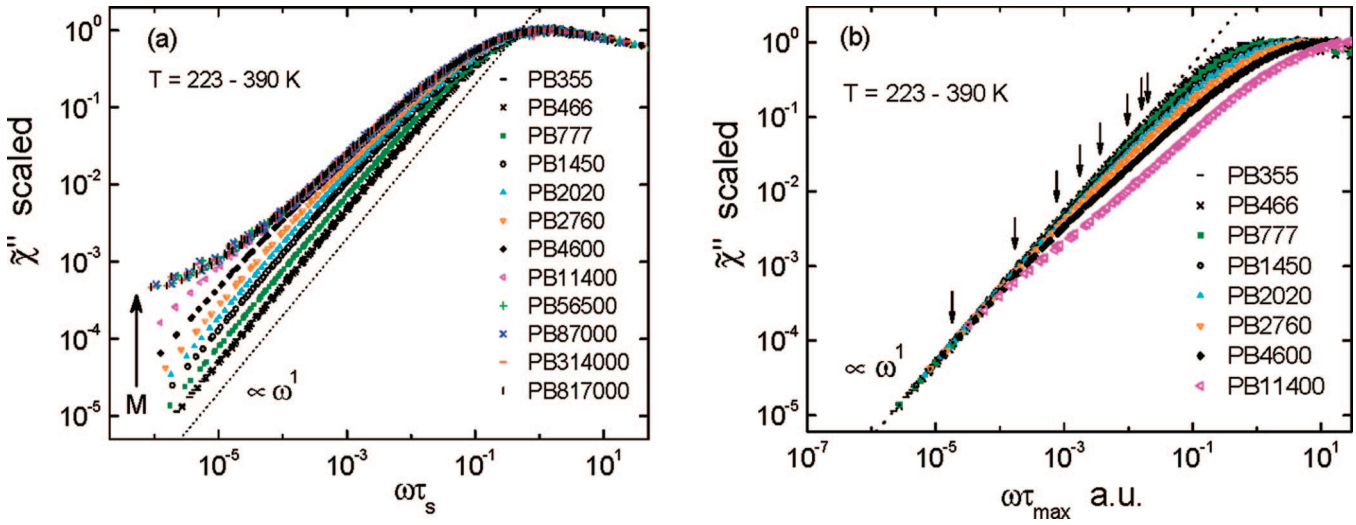

Figure 6. (a) Susceptibility master curves plotted as a function of reduced frequency $\omega\tau_s$ for the polybutadiene samples with different molecular weight M as indicated. (b) Susceptibility plotted as a function of reduced frequency $\omega\tau_{max}$ where τ_{max} (arrows) specifies the Rouse or terminal time; as a consequence all curves follow a common behavior at lowest frequencies.

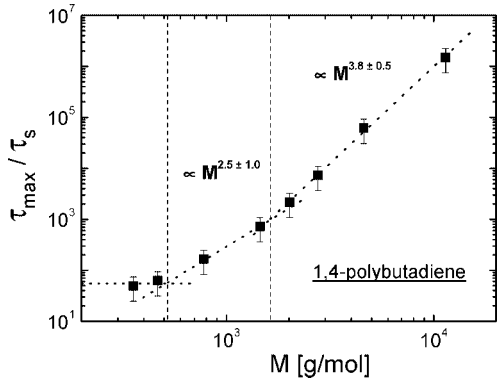

Figure 7. Ratio of maximal relaxation time τ_{max} over segmental time τ_s estimated from the crossover to low-frequency Debye behavior (cf. arrows in Figure 6b); three power law regimes are identified.

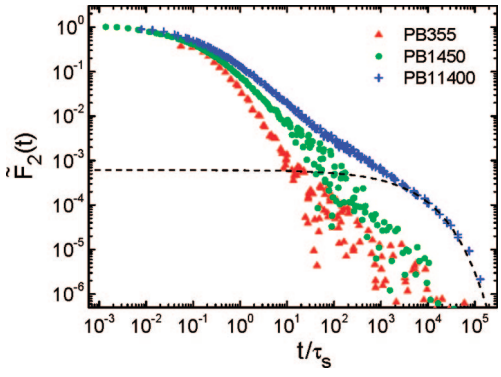

Figure 8. Reorientational correlation function vs reduced time t/τ_s for three polybutadienes, obtained from selected master curves of Figure 6a; dashed line gives an estimate of the plateau value associated with reptation dynamics.

corresponding to $S_e \cong 0.025$ (dashed line in Figure 8). In any case, FFC NMR allows to give a detailed picture of the reorientational correlation function covering glassy, Rouse, as well as reptation dynamics, which was not reported before.

B. Separating Polymer Spectra. As a next step of our analysis, we extract for each M the part of the total spectra of Figure 6a that is solely due to polymer dynamics ("polymer spectra"). According to eq 2, this is done by subtracting the

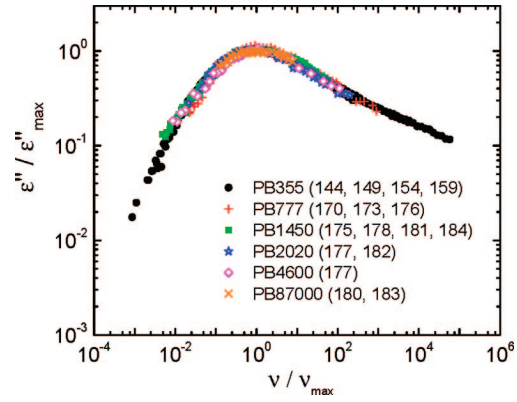

Figure 9. Master curve of the dielectric spectra of the 1,4-polybutadiene (PB) samples with different molecular weights; numbers in parentheses indicate temperature in K.

"glassy spectrum" of the low-M samples PB355 or PB466, the latter exhibiting no polymer-specific relaxation, from the total spectrum. This assumes that the glassy spectrum does not change with M, which is confirmed by the near M independence of the corresponding dielectric spectral shapes. This is shown in Figure 9, which displays dielectric spectra of different PB samples at several temperatures close to T_g, rescaled such that their maxima overlap. (Individual dielectric spectra were presented in paper I.) The rescaled spectra closely match, and thus their shape is approximately independent of temperature (FTS) and molecular weight. Since the dielectric spectra of PB, a type B polymer, are insensitive to polymer-specific effects[29,30] and thus only reflect glassy dynamics, we conclude that, to a good approximation, the latter is independent of molecular weight. This justifies the procedure of subtracting glassy dispersion spectra, as determined from low-M samples.

Figure 10 displays the "polymer spectra" of all samples, extracted by subtracting a "glassy contribution", as obtained from low-M spectra. The polymer spectra show a relaxation peak, whose magnitude grows with M. At $M > 4600$, the overall magnitude mostly saturates, although significant differences are still observed at low frequencies. Qualitatively, we interpret the spectra as fingerprints of emerging Rouse dynamics with growing chain length which, however, saturates at high M due to the onset of entanglement effects. The Rouse spectrum is first observed at $M = 777$, whereas its saturation occurs at M

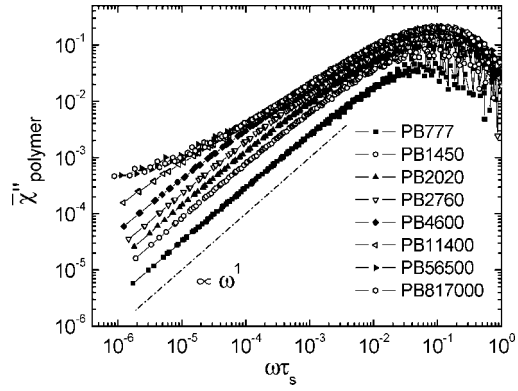

Figure 10. Separated spectra representing the polymer relaxation of a series of 1,4-polybutadiene samples with molecular weight M as indicated; dashed line represents power law behavior of a simple liquid.

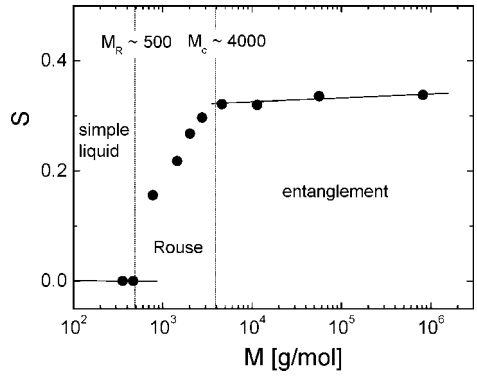

Figure 11. Dynamic order parameter S as a function of molecular weight M; solid line: guides to the eye; M_R and M_c denote the Rouse unit and entanglement molecular weight, respectively; dynamic regimes are indicated.

> 4600. In the frequency range $\omega\tau_s > 10^{-3}$, the spectra of entangled systems are almost indistinguishable from the essentially nonentangled $M = 4600$, indicating that the dynamics of entangled polymers at relatively high frequencies can still be described by Rouse modes. The qualitative spectral changes, observed at $M \geq 4600$ at the lowest reduced frequencies $\omega\tau_s < 10^{-3}$, signal the emergence of further retardation of the relaxation due to entanglement.

Recalling that the squared dynamic order parameter equals the relative weight of polymer dynamics in the total spectrum, $f = S^2$ (eq 2), we determine S^2 as the ratio of integrated intensities $\int\chi''(\omega)$ d ln ω of a polymer spectrum (Figure 10) and the corresponding total one (Figure 6a). Figure 11 shows the order parameter S as a function of M. The polybutadienes PB355 and PB466 do not exhibit polymer effects, and therefore their S is zero. Above $M = 466$, S first increases strongly, showing thereafter a trend to saturation above say $M \cong 4000$. It appears that the effective chain length does not grow above $M = 4000$. We take it as an indication that the system becomes entangled, so that Rouse dynamics are limited to chain segments between successive entanglements. Therefore, we estimate the crossover molecular weight, for which entanglements are fully established, as $M_c \cong 4000$. This is by a factor of about 2 larger than M_e, indicating first entanglement effects in Figure 7.

S reaches a maximal value $S_{max} = 0.34$. It appears that S_{max} is essentially determined by the Rouse dynamics, although a weak increase by $S_e \cong 0.02$ is observed within the range $4000 < M < 56\,500$. A value of $S_{max} = 0.34$ corresponds to $f = S^2 = 0.11$, which is much larger than usually reported in NMR literature.[3,4] We will come to this point again in the Discussion section. For the moment, we merely state that f can be decomposed into two parts due to Rouse and reptation dynamics and that according to our data the reptation contribution is rather small.

The polymer spectra displayed in Figure 10 also allow for testing the prediction of the Rouse theory. As described in section II, we numerically simulated Rouse spectra for series of chain lengths N (see Figure 1). There, the spectra appear as normalized spectra. Experimentally, we find that the (relative) spectral weight of the polymer spectra increases with M. This we explain by a growing chain length more and more impeding the isotropization of the local segmental dynamics—a fact not explained within standard Rouse theory. In order to allow for a direct comparison of their spectra shape, the polymer spectra in Figure 10 have thus to be normalized. We plot in Figure 12a the quantity $\tilde{\chi}''_{polymer}(\omega) = \bar{\chi}''_{polymer}(\omega)\pi/(2fI_{total})$, where I_{total} denotes the integral over each of the spectra in Figure 6a. By doing so, we guarantee that integrals over the polymer spectra are fixed to $\pi/2$ as are the calculated spectra. We only consider polymers with $M \leq 11\,400$ for which the terminal time of the polymer dynamics is essentially reached. Without significantly changing the height of relaxation maximum, the polymer spectra exhibit changes at low frequencies. This is expected as the evolving polymer dynamics lead to redistribution of spectral contributions at long times and low frequencies. At least for the molecular weights $M = 777$, 1450, 2020, and 2760 the behavior is similar to what is found within Rouse theory (cf. Figure 1b). Correspondingly, for comparison the calculated Rouse spectra for low N are again shown in Figure 12b. At low M and low N, high similarity between the experimental and theoretical polymer spectra is recognized; i.e., the intensity at lowest frequencies continuously increases. At $M > 2760$ a stronger increase is observed at low frequencies. Furthermore, one recognizes that all the experimental curves are significantly broader, indicating that the Rouse relaxation modes are not exponential but rather stretched, similar to the α-relaxation.

In Figure 13 we directly compare the shape of selected experimental polymer spectra with that of the calculated Rouse spectra. In order to allow such a comparison, experimental and calculated spectra were horizontally shifted to align at the maximum. Clearly, the calculated Rouse spectra with an exponential correlation function for each Rouse mode are too narrow. Using a stretched Kohlrausch decay $\exp(-(t/\tau)^\beta)$ in eq 4 with $\beta = 0.5$ results in a broader spectrum that better resembles the experimental spectra though systematic differences are still recognized. Thus, the particular shape of the Rouse mode spectra cannot be fully reproduced by Rouse theory.

According to eq 20, the magnitude of spectral density at the lowest frequencies $\omega\tau_s \ll 1$; i.e., the quantity $\tilde{J}_{polymer}$ is expected to exhibit a characteristic dependence on M as long as the Rouse model applies. Substituting $N = M/M_R$, one obtains

$$\lim_{\omega\tau_s \ll 1} \tilde{J}_{polymer}(\omega) = \lim_{\omega\tau_s \ll 1} \bar{\chi}''_{polymer}(\omega)/\omega = \tilde{J}_{Rouse}(0) \propto \log(M/M_R) \tag{24}$$

Equation 24 is expected to hold only in the high-M limit (cf. Figure 1a,b). In order to test more directly the Rouse theory result, expressed by eq 24, we first display in Figure 14a the experimental data of Figure 12a in the spectral density representation $\tilde{J}_{polymer}(\omega) = \tilde{\chi}''_{polymer}(\omega)/\omega$. We remind the reader that the spectral density $\tilde{J}(\omega) \propto 1/T_1(\omega)$ is essentially the quantity measured in a FFC NMR experiment. For the PB samples with $M \leq 4600$, the spectral density levels off (becomes flat) at low frequencies, so that it is possible to approximate $\tilde{J}_{polymer}(0)$ as the magnitude at the lowest accessible frequency. At $M > 4600$, the low-frequency spectrum is not flat, yet a lower bound of $\tilde{J}_{polymer}(0)$ may still be given for $M = 11\,400$ where a crossover

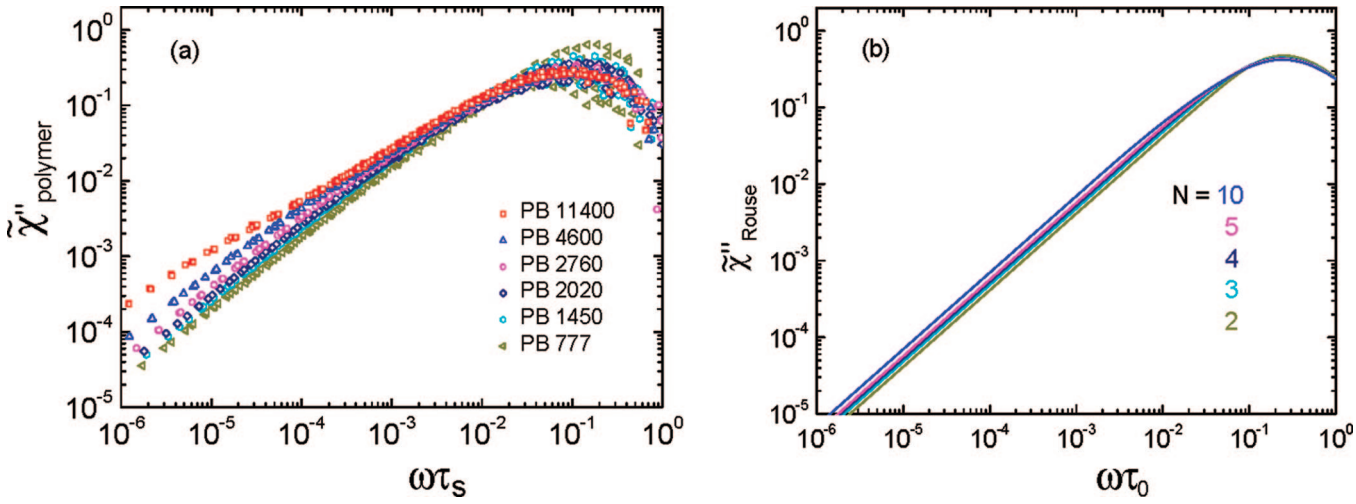

Figure 12. (a) Normalized experimental polymer susceptibility spectra for 1,4-polybutadiene (PB) samples with $M \leq 11\,400$; note that the spectra of PB11400 and PB4600 reflect already the influence of entanglement. (b) Calculated Rouse spectra for chain lengths N as indicated.

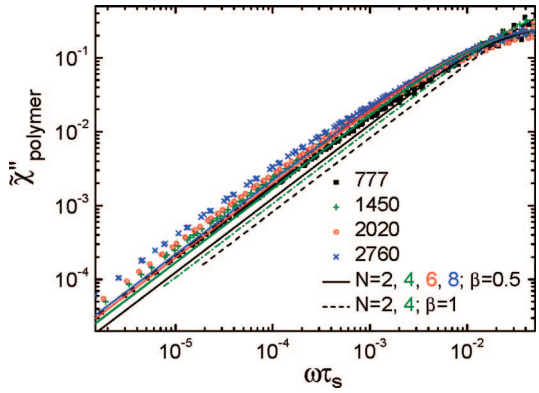

Figure 13. Comparison of the normalized polymer spectra with calculated Rouse spectra applying a Debye ($\beta = 1.0$, dashed lines) and a Kohlrausch decay function ($\beta = 0.5$, full lines).

to a flat spectral density may be still anticipated. In Figure 14b, the value of $\tilde{J}_{polymer}(\omega)$ at lowest accessible frequency is compared to $\tilde{J}_{Rouse}(0)$, expected from the Rouse theory, eq 20. Using $M_R = 500$, as assumed above, a similar trend can only be reached for the first three polymers with $M = 777$, 1450, and 2020. We note that as we do compare equally normalized spectra no scaling factor is involved for getting the agreement at low M in Figure 14b. At higher M, strong deviations from the initial linear behavior (line) expected from Rouse theory are observed. Thus, already at $M = 2000$ there appear first signs of entanglement and reptation effects that give rise to an additional contribution to the spectral density at low frequencies, in excess of the Rouse spectrum. Tentatively, we identify $M = 2000$ with an entanglement weight M_e which is actually by a factor of 2 smaller than the entanglement weight M_c observed above (cf. Figures 7 and 11). Here a comment is worthwhile. Clearly, the agreement in Figure 14b can be improved if we make M_R by a factor 2 smaller, and one can argue that indeed defining M_R is somewhat ambiguous since at lowest values of N the description of a polymer chain by discrete beads becomes artificial. By its meaning, M_R corresponds to one Rouse segment. The molecular weight of the Rouse segment was determined to be ~500 since the sample with $M = 466$ does not show any deviation of the susceptibility spectrum from that of the low molecular weight sample and of OTP, while the $M = 777$ sample already shows some excess at low frequencies. On the other hand, formally one Rouse segment consist of two beads and one mass less spring, so one Rouse bead has mass equal to ≅250. With the value $M_R = 250$ the agreement between experimental data for $\tilde{J}_{polymer}(0)$ and the Rouse expectation is better than in the case $M_R = 500$ (Figure 14b). The experimental susceptibility spectrum would then correspond to higher values of N; e.g., $M = 1450$ and 2020 will correspond to $N = 6$ and 8, respectively.

C. Molecular Weight Dependence of the Glass Transition Temperature T_g. Finally, we discuss the molecular weight dependence of the glass transition temperature $T_g(M)$. Glass transition temperature is usually associated with a structural relaxation time of 100 s. Defining thus T_g as the temperature at which the dielectric relaxation time is $\tau_\alpha = \tau_s = 100$ s (cf. Figure 5), we display the function $T_g(M)$ in Figure 15. In addition we included the M dependence of the parameter T_0 of the Vogel−Fulcher−Tammann equation, $\tau_s \propto \exp(D/(T - T_0))$. Clearly, for both quantities T_g and T_0 one can identify three regimes, separated by M_R and M_e as obtained from the NMR analysis. The strong M dependence at $M < M_R$, typical of low molecular weight glass-formers, becomes weaker in the Rouse regime and finally saturates in the entanglement regime. This behavior quite disagrees with most literature results on the subject, where $T_g(M)$ is usually discussed in terms of a smooth dependence that follows from the free-volume theory[16,17] (cf. Discussion section).

V. Discussion

Several years ago, a FFC NMR investigation of 1,4-polybutadiene (PB) was reported in the literature.[3,4,26] Compared to that work, we cover significantly wider ranges of temperatures and molecular weights, focusing, in particular, on the transition from simple liquid to polymer melt. More importantly, we use a rather different approach to the data analysis. In contrary to the usual practice, we suggest that the NMR relaxation data are best analyzed in the susceptibility representation, which favors comparisons with the results of other techniques and also facilitates relaxation data analyses and their decomposition into physically distinct contributions. We show that an accurate analysis of characteristic polymer spectra is only possible when the (much stronger) underlying glassy dynamics is properly accounted for. For this separation we essentially follow the "different time scale approach" discussed by Kimmich and Fatkullin.[3] Only after having extracted polymer contributions from the total spectra does their quantitative analysis within Rouse theory become possible. A precondition for performing such an analysis is the validity of frequency temperature superposition which allows us to combine relaxation spectra,

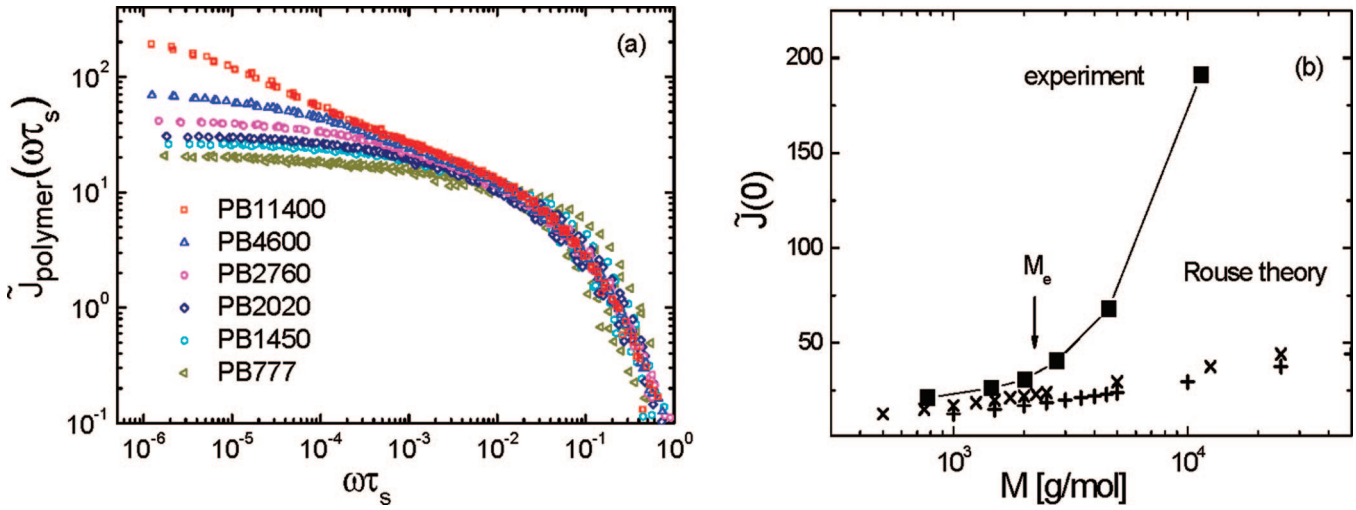

Figure 14. (a) Polymer spectral density (obtained from data in Figure 12a) as a function of reduced frequency for selected polybutadienes, as indicated. (b) Spectral density at lowest experimentally accessed frequency (cf. (a)) as a function of molecular mass and comparison with Rouse theory (straight lines). Squares: experimental data. Plus and crosses correspond to $M_R = 500$ and 250, respectively. M_e indicates mass of onset of entanglement.

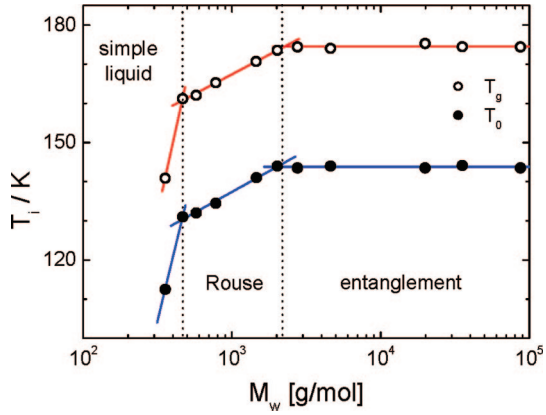

Figure 15. Glass transition temperature T_g as a function of molecular weight M determined from dielectric spectroscopy. Three regimes are identified separated by the molecular weight of the Rouse unit M_R and the weight of the onset of entanglement M_e. For comparison, the parameter T_0 of the VFT equation is shown.

displayed as functions of $\omega\tau_s$, into master curves covering a broad range of frequencies. We are aware that, in order to single out the polymer spectra, instead of subtracting the glassy contribution from the total relaxation spectrum, a mathematical deconvolution would be more appropriate since a strict time scale separation of Rouse and glassy dynamics is not always fully given. However, we think the results will not significantly be altered, but this has to be checked in future work.

Our analysis provides a wealth of new results, unknown from previous NMR work, namely, the molecular weight of a Rouse unit $M_R \cong 500$; the characteristic crossover molecular weight $M_e \cong 2000$ at which the first entanglement effects are observed; the order parameter and its molecular weight dependence $S(M)$; the molecular weight dependence of terminal time $\tau_{max}(M)$; and, last but not least, the temperature dependence of the segmental relaxation time $\tau_s(T)$. The latter agrees well with the corresponding dielectric relaxation times and can be identified with the time scale of the α-process, i.e., $\tau_s = \tau_\alpha$. Our results for M_R and M_e are in accordance with the data from other techniques.[31–34] For example, a ^{2}H NMR study[31] estimated $M_R \cong 250$ and $M_e \cong 2000$, whereas $M_e \cong 1600$ was estimated from rheological studies.[34] We reiterate that the low-M PB samples with $M = 355$ and 466 do not exhibit polymer-specific effects but rather behave as simple molecular liquids. Thus, we detect the transition from a simple liquid to a polymer melt at higher M with respect to what is expected from the Kuhn element weight.[35] However, we repeat that within the Rouse analysis M_R can equally well be defined as 500/2, and in all statements regarding the number N of Rouse modes appearing a factor 2 could be justified.

On the basis of the analysis of preceding sections, the following picture emerges for PB. At low M, below the characteristic Rouse unit size M_R, the linear structure of (flexible) chains appears immaterial for their relaxation dynamics, the latter resembling the behavior of, e.g., monomeric *o*-terphenyl (cf. paper I). All possible internal degrees of freedom of a flexible molecule with $M < M_R$ appear to be merged into a single relaxation peak attributed to glassy dynamics with a time constant $\tau_s \cong \tau_\alpha$. Note also that the dielectric spectra of PB are virtually M-independent (cf. Figure 9). Increasing the molecular weight beyond M_R brings about additional relaxation processes, which can be understood in terms of emerging Rouse modes, the latter growing in number with increasing chain length. Eventually, the polymer chains of increasing lengths become entangled, so that on the time scale of Rouse relaxation the chain segments of a characteristic size M_c effectively become "pinned down" at the entanglement points. Then, the number of Rouse modes cannot grow any more, since the number of participating Rouse segments is effectively limited to $N_c = M_c/M_R$. At still higher M, the entanglements are fully established, and therefore Rouse dynamics remains basically unchanged, whereas the increasingly slow reptations eventually bring about the ultimate polymer relaxation. On the basis of our current results, we determine the characteristic entanglement weight of polybutadiene as $M_c \cong 4000$ and consequently the corresponding maximal Rouse chain length, i.e. the "mesh size", as $N_c \cong 8$. However, we observe certain entanglement effects already at $M_e \cong 2000$, i.e., at $N_e = M_e/M_R \cong 4$. Here, a factor 2 appears between M_c and M_e as in the case of comparing the crossover molecular weight from viscosity and modulus data, respectively.[6]

As said, the effective Rouse chain length is limited by the mesh size of the entanglement, so that increasing the chain beyond that limit does not lead to increased number of Rouse modes. In PB of high M, we can only estimate a maximum of $N \cong 8$ Rouse modes, which yet give rise to a broad spectrum over about 3 decades at $\omega\tau_s < 1$. Thus, the limiting Rouse spectrum for (infinitely) high number of modes N is never reached in an equilibrium polymer melt, since entanglement

effectively limits N. Instead of testing the expected limiting behavior (eq 22), one rather has to perform a detailed Rouse analysis, accurately summing up a small number of Rouse modes. Correspondingly, the often discussed limiting Rouse spectrum of the shear modulus,[5,6,36] $G''(\omega) \propto \omega^{1/2}$, is not expected to show up, either. Indeed, MD simulation showed that full Rouse spectrum cannot be established, as entanglement effects set in before,[37,38] leading to an apparent exponent somewhat higher than 1/2. The introduction of a stretched rather than simple exponential relaxation of Rouse modes improves their agreement with the experimental data, a fact also known from simulation work.[37–39]

In contrast to our previous conclusion,[2] the increase of $S(M)$ cannot be explained by standard Rouse theory. There the calculated Rouse spectra were not correctly normalized. Thus, theoretical efforts are needed to explain the characteristic increase of $S(M)$ in the Rouse regime. Moreover, the high M limit, $S_{max} = 0.34$, is significantly larger than usually reported and is essentially reached already in the Rouse regime, while the additional increase S_e by reptation effects is relatively small. Already the Rouse dynamics leads to a strong spatial restriction of the segmental dynamics which strongly grows with M until reaching M_c, but is only weakly enhanced by the entanglement dynamics. Thus, the values of S discussed here must not be compared with the values estimated from the influence of entanglement and reptation effects. In a double quantum (DQ) NMR study of entangled PB, Spiess and co-workers[13,14] monitored the segmental correlation function at long times, comparing the results with the predictions of reptation model.[40] From the plateau in the correlation function, they determined the order parameter S and reported values as high as $S = 0.2$ in linear PB, even higher in block copolymers,[14] and however somewhat smaller values in PB polymer networks.[41] At first sight, these results of large S appear to agree with ours, as we indeed concluded in our initial study.[2] A closer inspection reveals, however, that the apparent agreement is misleading. Our results suggest that the main contribution to S comes from Rouse dynamics, whereas the part due to entanglement and reptation effects is rather small, $S_e \cong 0.02$. The mentioned works, however, deduced their high S from the height of the entanglement plateau of segmental correlation function, and thus their (large) S has to be compared with our (small) S_e, the two results obviously disagreeing. Instead, our result of small $S_e \cong 0.02$ is essentially in agreement with theoretical estimates[14,36,42] and with previous experimental results[43,44] and also agrees with the estimate obtained from Figure 8 where the full orientational correlation functions are shown, yielding an indication of a plateau for $M = 11\,400$, which we have estimated to be $S_e = 0.025$. In addition, we reiterate that the order parameter as determined by NMR is not necessarily related to orientational structural order (see paper I). We note that the unusual high chain order parameters observed by DQ NMR were recently explained by incomplete segmental averaging in the sense that the Rouse relaxation may not have completely decayed in the respective time window of DQ NMR.[41,45]

As discussed by Spiess and co-workers,[13,14] the experimentally determined order parameter S depends on the direction of the considered proton pair vector with respect to the direction of the chain contour and generally is smaller than the actual order parameter of the chain itself. It is the virtue of DQ NMR to allow a selected proton pair to be probed. Consequently, DQ NMR identified quite different values of S for the different proton pairs in PB.[14] Regarding FFC NMR, a selection of particular protons is not easily possible, so that one determines averaged dynamics over all relevant spin pairs in the monomer. The quite different overall dispersion behavior of polyisoprene with respect to that of PB[46] could be explained by assuming a much smaller order parameter S and, as a consequence, a much larger influence of the glassy dynamics in the overall NMR spectra.

The correlation function of PB11400 exhibits only some indication of bimodal decay (see Figure 8). A clear-cut plateau was not detected in simulations, either.[47] However, it may be expected that at sufficiently high M the reptation dynamics become so slow that they do not lead to a decay of correlations at intermediate times, so that there appears a plateau. Regarding Rouse relaxation, however, one does not expect a well-defined correlation step, separated by a plateau, but rather a continuous broadening of the main relaxation peak on the low-frequency side, since relaxation times of Rouse modes spread over the range $\tau_s < \tau_p < \tau_R$ (see also simulation results in Figure 1b).

Recently, Ding et al.[48] argued that the molecular weight dependence of T_g depends on the molecular weight m_R of the "random step" which is different from what is usually taken for the Kuhn element. Basically, the findings of the present paper support this idea, and m_R may be identified with the present Rouse unit mass M_R, and we find that for PB this random step is ~500, about 2 times larger than the Kuhn segment weight of PB.[35] However, in the case of PB we cannot confirm another suggestion of the authors, namely that the saturation of the $T_g(M)$ dependence occurs when a chain reaches Gaussian statistics; i.e., it is argued that M_e does not play a role for the $T_g(M)$ dependence; instead, $T_g(M)$ is assumed to show a smooth function on M. In our $T_g(M)$ data, clearly distinct dependencies on M in the Rouse and entanglement regime are observed (Figure 15); in particular, $M_e \sim 2000$ marks the saturation point for T_g, while the Gaussian statistics is expected to be displayed roughly at $M \geq 10M_R \sim 5000$ in the case of PB. We note that experimental data for the molecular weight dependence of T_g exhibit strong scatter in most cases, and thus it is difficult to determine reliably which weight corresponds to the saturation of T_g; a factor of 2 for this weight is normally within the accuracy of the data. We note that kinks in the $T_g(M)$ curves were also reported by Cowie for several polymers.[18]

Concluding, the results compiled in the present paper as well as in part I demonstrate that FFC NMR relaxometry is a powerful tool for characterizing the dynamics in polymer melts. With the help of FTS master curves are attainable which cover about 8 decades in frequency. With extending the measurements to even higher temperatures and pushing the FFC method to its low frequencies limits (say 100 Hz−1 kHz, by applying appropriate earth and stray field compensation) even 10−11 decades broad spectra appear feasible.[49] Thus, the polymer dynamics, including Rouse as well as reptation dynamics, may be completely monitored, and attempts to find the full orientational relaxation function will be undertaken as has been done in the case of viscoelastic experiments.[50–52] Moreover, performing the analysis in the susceptibility representation the relationship of orientational dynamics and shear stress relaxation, for example, may be addressed in detail. Not taking into account the glassy dynamics contribution, an analysis of NMR relaxation data on polymer melts may be misleading, in particular, in the Rouse regime. Future theory has to explain the redistribution of polymer and glassy dynamics reflected in the increase and saturation of the quantity $S(M)$ in the Rouse and entanglement regime, respectively. Actually, a unified glass-and-polymer theory is needed.

Acknowledgment. The authors thank S. Stapf for supplying the high molecular weight polybutadiene samples ($M = 56\,500$, 87 000, 314 000, and 817 000). Also, fruitful discussions with N. Fatkullin are appreciated. Support of Deutsche Forschungsgemeinschaft (DFG) through SFB 481 is highly acknowledged.

References and Notes

(1) Kariyo, S.; Brodin, A.; Gainaru, C.; Herrmann, A.; Schick, H.; Novikov, V. N.; Rössler, E. A. *Macromolecules* **2008**, *41*, 5313–5321.
(2) (a) Kariyo, S.; Gainaru, C.; Schick, H.; Brodin, A.; Novikov, V. N.; Rössler, E. A. *Phys. Rev. Lett.* **2006**, *97*, 207803-1–207803-4. (b) Erratum: Kariyo, S.; Herrmann, A.; Gainaru, C.; Schick, H.; Brodin, A.; Novikov, V. N.; Rössler, E. A. *Phys. Rev. Lett.* **2008**, *100*−1.
(3) Kimmich, R.; Fatkullin, N. *Adv. Polym. Sci.* **2004**, *170*, 1–113.
(4) Kimmich, R.; Anoardo, E. *Prog. NMR Spectrosc.* **2004**, *44*, 257–320.
(5) Doi, M.; Edwards, S. F. *The Theory of Polymer Dynamics*; Oxford Sci. Publication: New York, 1986.000
(6) McLeish, T. C. B. *Adv. Phys.* **2002**, *51*, 1379–1527.
(7) Angell, C. A.; Ngai, K. L.; Mckenna, G. B.; McMillan, P. F.; Martin, S. W. *J. Appl. Phys.* **2000**, *88*, 3113–3157.
(8) Lunkenheimer, P.; Schneider, U.; Brand, R.; Loidl, A. *Contemp. Phys.* **2000**, *41*, 15–36.
(9) Blochowicz, T.; Brodin, A.; Rössler, E. A. *Adv. Chem. Phys.* **2006**, *133 Part A*, 127–256.
(10) Bloembergen, N.; Purcell, E. M.; Pound, R. V. *Phys. Rev.* **1948**, *73*, 679–715.
(11) Abragam, A. *The Principles of Nuclear Magnetism*; Clarendon: Oxford, 1961.
(12) Lipari, G.; Szabo, A. **1982**, *104*, 4546–4559.
(13) Graf, R.; Heuer, A.; Spiess, H. W. *Phys. Rev. Lett.* **1998**, *80*, 5738–5741.
(14) Dollase, T.; Graf, R.; Heuer, A.; Spiess, H. W. *Macromolecules* **2001**, *34*, 298–309.
(15) Callaghan, P. T.; Samuski, E. T. *Macromolecules* **2000**, *33*, 3795–3802.
(16) Fox, T.; Flory, P. J. *J. Polym. Sci.* **1954**, *14*, 315–319.
(17) Ueberreiter, K.; Kanig, G. *J. Colloid Sci.* **1952**, *7*, 569–583.
(18) Cowie, J. M. G. *Eur. Polym. J.* **1975**, *11*, 297–300.
(19) Rouse, P. J. *J. Chem. Phys.* **1953**, *21*, 1272–1280.
(20) Bueche, F. *J. Chem. Phys.* **1953**, *22*, 603–609.
(21) Verdier, P. H. *J. Chem. Phys.* **1966**, *45*, 2118–2121.
(22) Rubinstein, M.; Colby, R. H. *Polymer Physics*; University Press: Oxford, 2005.
(23) Khazanovich, T. N. *Polym. Sci. USSR* **1963**, *4*, 727–736.
(24) Ullman, R. *J. Chem. Phys.* **1965**, *43*, 3161–3177.
(25) Fatkullin, N.; Kimmich, R.; Weber, H. W. *Phys. Rev. E* **1993**, *47*, 4600–4603.
(26) Kimmich, R.; Fatkullin, N.; Seiter, R.-O.; Gille, R. *J. Chem. Phys.* **1998**, *108*, 2173–2177.
(27) Plazek, D. J. *J. Rheol. (N.Y.)* **1996**, *40*, 987–1014.
(28) Ding, Y.; Sokolov, A. P. *Macromolecules* **2006**, *39*, 3322–3326.
(29) Stockmayer, W. H. *Pure Appl. Chem.* **1967**, *15*, 539–554.
(30) Kremer, F., Schönhals, A., Eds.; *Broadband Dielectric Spectroscopy*; Springer: Berlin, 2003.
(31) Klein, P. G.; Adams, C. H.; Brereton, M. G.; Ries, M. E.; Nicholson, T. M.; Hutchings, L. R.; Richards, R. W. *Macromolecules* **1998**, *31*, 8871–8877.
(32) Doi, M. In *Material Science and Technology*; Verlag Chemie: Weinheim, 1993; Vol. *12*, p 389.
(33) Cho, K. S.; Ahn, K. H.; Lee, S. J. *J. Polym. Sci., Part B: Polym. Phys.* **2004**, *42*, 2724–2729.
(34) Liu, C.; He, J.; Keunings, R.; Bailly, C. *Macromolecules* **2006**, *39*, 3093–3097.
(35) Brandrup, J., Immergut, E. H., Eds.; *Polymer Handbook*, 2nd ed.; Wiley-Interscience: New York, 1975.
(36) Ferry, J. D. *Viscoelastic Properties of Polymers*, 3rd ed.; Wiley: New York, 1980.
(37) Bennemann, C.; Baschnagel, J.; Paul, W.; Binder, K. *Comput. Theor. Polym. Sci.* **1999**, *9*, 217–226.
(38) Padding, J. T.; Briels, W. J. *J. Chem. Phys.* **2001**, *114*, 8685–8693.
(39) Kreer, T.; Baschnagel, J.; Müller, M.; Binder, K. *Macromolecules* **2001**, *34*, 1105–1117.
(40) Ball, R. C.; Callaghan, P. T.; Samulski, E. T. *J. Chem. Phys.* **1997**, *106*, 7352–7361.
(41) Saalwächter, K.; Herrero; B.; Lopez-Manchado, M. A. *Macromolecules* **2005**, *38*, 9650–9660.
(42) Kuhn, W.; Grün, F. *Kolloid Z.* **1942**, *101*, 248–271.
(43) Cohen-Addad, J. P. *J. Chem. Phys.* **1975**, *63*, 4880–4885.
(44) Collignon, J.; Sillescu, H.; Spiess, H. W. *Colloid Polym. Sci.* **1981**, *259*, 220–226.
(45) Saalwächter, K.; Heuer, A. *Macromolecules* **2006**, *39*, 3291–3303.
(46) Kariyo, S.; Stapf, S. *Macromolecules* **2002**, *35*, 9253–9255.
(47) Faller, R.; Müller-Plathe, F.; Heuer, A. *Macromolecules* **2000**, *33*, 6602–6610.
(48) Ding, Y.; Kisliuk, A.; Sokolov, A. P. *Macromolecules* **2004**, *37*, 161–166.
(49) Gainaru, C.; Lips, O.; Troshagina, A.; Kahlau, R.; Brodin, A.; Fujara, F.; Rössler, E. A. *J. Chem. Phys.* **2008**, in press.
(50) Colby, R. H.; Fetters, L. J.; Graessley, W. W. *Macromolecules* **1987**, *20*, 2226–2237.
(51) Baumgaertel, M.; De Rosa, M. E.; Machado, J.; Masse, M.; Winter, H. H. *Rheol. Acta* **1992**, *31*, 75–82.
(52) Benallal, A.; Marin, G.; Montfort, J. P.; Derail, C. *Macromolecules* **1993**, *26*, 7229–7235.

MA702758J